

Article

Performance Analysis of Two-Hop mmWave Relay Nodes over the 5G NR Uplink Signal

Randy Verdecia-Peña ^{1,2,*}  and José I. Alonso ^{1,2} 

¹ Information Processing and Telecommunications Center, Universidad Politécnica de Madrid, 28040 Madrid, Spain; ignacio@gmr.ssr.upm.es

² ETSI de Telecomunicación, Universidad Politécnica de Madrid, 28040 Madrid, Spain

* Correspondence: randy.verdecia@upm.es

Abstract: In this paper, the uplink in a two-hop 5G new radio co-operative system using Relay Nodes (RNs) in millimeter bands has been simulated and studied. We focus on an uplink Amplify-and-Forward Relay Node (A&F RN) and Decode-and-Forward Relay Node (D&F RN) with an mmWave-band transceiver chain (Tx/Rx). We study two uplink mmWave MIMO D&F relaying protocols assuming, firstly, the complete knowledge of the uplink channel and, secondly, the uplink channel estimation through a Least Square (LS) algorithm. To verify the benefits of the proposed uplink mmWave MIMO co-operative network, a link-level co-operative simulator has been developed using MatlabTM and SimulinkTM software, where an indoor-to-outdoor scenario and mmWave transceiver with off-the shelf components are considered. The main novelty of this link-level co-operative simulator and the implemented relay nodes is the usage of signals with 5G NR features, such as UL-SCH transport channel coding and PUSCH generation, which are the other main contributions of this article. Based on the numerical results in terms of the achievable Bit Error Rate (BER) and throughput, we show that the two-hop uplink co-operative network substantially improves the performance in the communications between the NR-User Equipment (NR-UE) and the logical 5G Radio Node (gNodeB). For example, the results from using uplink mmWave NR-D&F protocols far exceed those achieved with the uplink mmWave NR-A&F algorithm; in the case of the 64-QAM modulation scheme for the SISO technique, an improvement of 6.5 Mbps was achieved using the D&F PCE protocol, taking into account that the 256-QAM constellation is higher by 4.05 Mbps. On the other hand, an average throughput enhancement of 28.77 Mbps was achieved when an uplink mmWave ($2 \times 4 \times 4$) D&F PCE strategy was used versus an uplink mmWave SISO D&F LS protocol for a Signal-to-Noise Ratio (SNR) = 20 dB and 64-QAM signal. However, an improvement of 56.42 Mbps was reached when a 256-QAM modulation scheme was employed. Furthermore, this paper introduces the first study to develop an uplink mmWave MIMO 5G co-operative network platform through a Software Defined Radio (SDR) from a practical implementation point of view.



Citation: Verdecia-Peña, R.; Alonso, J.I. Performance Analysis of a Two-Hop mmWave Relay Nodes over the 5G NR Uplink Signal. *Appl. Sci.* **2021**, *11*, 5828. <https://doi.org/10.3390/app11135828>

Academic Editor: Mario Marques Da Silva

Received: 26 May 2021

Accepted: 20 June 2021

Published: 23 June 2021

Publisher's Note: MDPI stays neutral with regard to jurisdictional claims in published maps and institutional affiliations.



Copyright: © 2021 by the authors. Licensee MDPI, Basel, Switzerland. This article is an open access article distributed under the terms and conditions of the Creative Commons Attribution (CC BY) license (<https://creativecommons.org/licenses/by/4.0/>).

Keywords: millimeter-wave MIMO; uplink 5G NR; relay node cooperative system

1. Introduction

In recent years, several solutions have been studied, proposed, and standardized to reach the demanded requirements of New Generation Mobile Communications (5G), which is expected to provide more capacity and connect more smart devices compared with the current networks [1]. In this sense, Multiple-Input Multiple-Output (MIMO), Millimeter-Wave (mmWave), Carrier Aggregation (CA), and relaying techniques have been received attention from the academy and industrial sectors [2–4]. Firstly, the MIMO technique has been extensively employed in wireless communications and the current mobile communication systems due to it being able overcome the single-antenna system Shannon capacity. Nevertheless, the number of users in the communication networks has increased rapidly in recent years, which means that the New Radio (NR) wireless networks

should require higher data rates, robustness, spectral efficiency, etc. Among the scenarios for 5G, mobile and wireless communications are expected: Direct Device-to-Device (D2D) communication [5], Massive Machine Communication (MMC) [6], Moving Networks (MNs) [7], Ultra-Dense Networks (UDNs) [8] and Ultra-Reliable Communication (URC) [9]. In order to solve the limitation of spectrum resources, the spectrum-rich mmWave has received special attention as the key spectrum of 5G and future technologies as 6G [10].

The wide spectrum available in millimeter bands [11] makes millimeter-wave technology an enabling technology for the deployment of 5G networks. It would provide a solution to address the challenges of bandwidth scarcity in 5G systems. However, the main challenge of the mmWave bands is undergone by the very high propagation loss, which substantially limits the communication distance in comparison with the FR1 frequency bands (<6 GHz) of 5G. For example, the free space path loss of a 20-m link at 60 GHz frequency can easily exceed 90 dB. On the other hand, thanks to the smaller wavelengths, it is easier to implement hardware massive MIMO (mMIMO) [12] systems, which can compensate for some of the limitations of millimeter band propagation. Consequently, millimeter waves and massive MIMO can be combined to achieve the maximum performance of both technologies [13–15]. In addition, it has been demonstrated that the co-operative networks using Relay Nodes (RNs) increase capacity and network coverage as well as decrease the path loss and total transmission power [16]. In conclusion, the combination of relay node co-operative networks and MIMO in mmWave bands emerges as an optimal solution to address the requirements of 5G network deployments.

Our investigation team has been deeply studying the co-operative networks in this context; in [17], a MIMO relay node co-operative system based on Software Defined Radio (SDR) and Matlab™ software is implemented over the downlink LTE signal. Additionally, ref. [18] implements a link-level co-operative simulator for the study of mmWave MIMO RNs over the downlink 5G signal. However, the implementation of the mmWave MIMO RN co-operative network over 5G uplink has not been studied and evaluated yet. Therefore, in this work, we consider the first step to the implementation of mmWave MIMO co-operative network for the 5G uplink signal. Motivated by the described issues, in this paper, an mmWave MIMO 5G relay node co-operative system over a 5G uplink through Matlab™ and Simulink™ tools has been implemented and evaluated. In this paper, the major contributions are summarized as follows:

- A link-level co-operative simulator for an uplink two-hop network using out-band 5G RNs at mmWave frequency and with MIMO capabilities is proposed and implemented.
- In the proposed co-operative system, the 5G NR signal features, UL-SCH transport channel coding, and PUSCH generation were implemented, which fulfilled the requirements of the NR uplink 3GPP.
- Decode-and-Forward (D&F) protocols taking into account the channel knowledge with a Perfect Channel Estimation (PCE) and Least Square (LS) estimator were developed. Additionally, both structures implement the Minimum Mean Square Error (MMSE) equalization technique. Furthermore, analytical expressions for the D&F strategy of the proposed uplink co-operative network were derived.
- An Amplify-and-Forward (A&F) strategy has been developed. Furthermore, system models for both A&F and D&F relaying strategies of the proposed uplink mmWave MIMO relay node co-operative network with a real-world focus have been derived.
- In addition, the authors focus on the study in an indoor-to-outdoor scenario, using the 64-QAM and 256-QAM modulation schemes. Additionally, extensive simulations were taken into account and carried out with the Matlab™ and Simulink™ tools, considering the non-linearity of mmWave subsystems.

The rest part of this paper is structured as follows. Section 2 provides the system model and basic assumptions, in which uplink mmWave A&F and uplink mmWave D&F relays are introduced. In Section 3, the link-level co-operative simulator, topology, channel model, and mmWave transceptor are explained. The simulation results and performance

evaluation are presented and discussed in Section 4. Finally, the conclusions are drawn in Section 5.

Notation: Boldface lower and upper case symbols represent vectors and matrices, respectively. $(\cdot)^H$ denotes the Hermitian transpose of a vector or a matrix. $\|\cdot\|_F$ is the Forbenius norm and $N \sim (m, \sigma^2)$ describes a complex Gaussian random variable with mean m and variance σ^2 .

2. System Model and Basic Assumptions

In this section, we will describe both the relay node architecture and its implementation. First of all, the signal model of the proposed relays in this article will be explained. A&F and D&F relay nodes deal with different signal models. Additionally, the advantages and the main differences between both schemes will be highlighted. Then, the implementation of a link-level co-operative simulator using MatlabTM and SimulinkTM software will be explained. Figure 1 shows a two-hop uplink mmWave MIMO NR-RN system model in a wireless network. The architecture consists of one source node (NR-UE), an intermediate node (NR-RN protocol), and a destination node (gNodeB) working in a Half Duplex (HD).

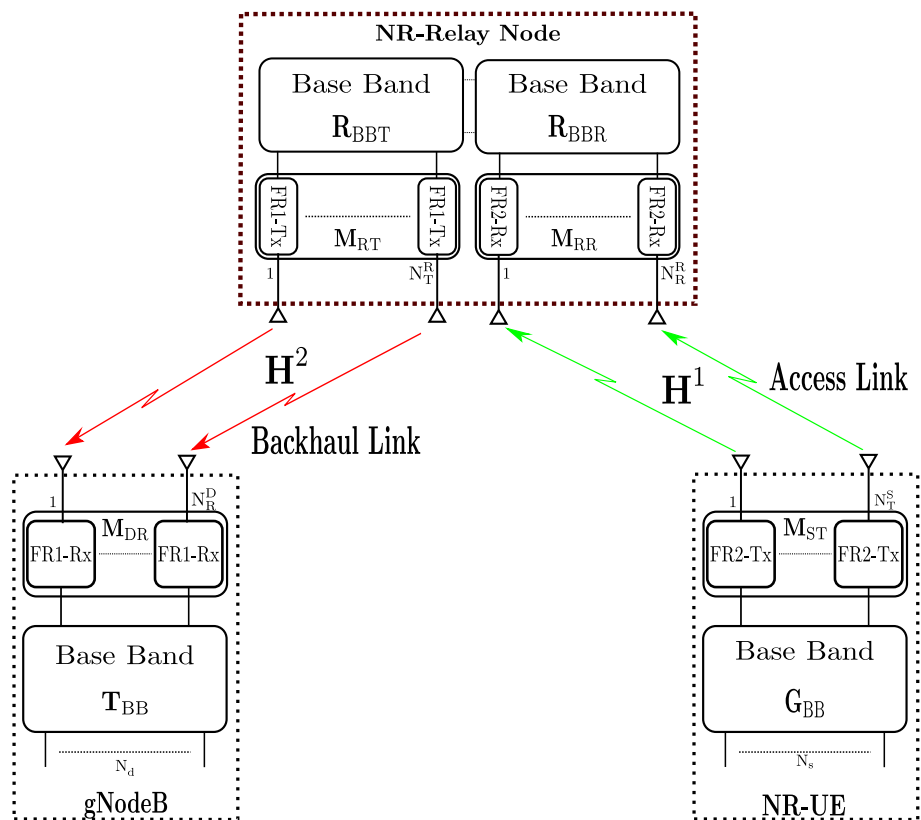


Figure 1. Uplink mmWave MIMO New Radio (NR)-relay node architecture.

From Figure 1, it can be seen that the NR-UE node includes two blocks: the baseband signal processing block and an array of transmitter chains in the 5G FR2 (26 GHz) band (FR2-Tx). In this architecture, an essential node is the new radio relay node, which comprises an array of receiver chains in mmWave (FR2-Rx), where its function is to convert the 5G FR2 frequency band to baseband. Furthermore, the baseband signal processing block involves two blocks, receiver and transmitter baseband signal processing, which are described, respectively, through R_{BBR} and R_{BBT} matrices. Finally, the third block in the NR-RN strategy contains an array of FR1-Tx to up-convert the baseband signal to the 5G FR1 (3.5 GHz) frequency band, which, in our link-level co-operative simulator, was implemented by means of Universal Software Radio Peripheral (USRP). On the other hand, the gNodeB includes two blocks: the baseband processing block (T_{BB}) and an array of RF Chains (FR1-

Rx) to down-convert the 3.5 GHz to the baseband frequency band. It should be noted that, in this paper, the direct link between the source and destination, is not studied because it is considered to operate in different band frequencies.

We consider an uplink mmWave co-operative Single-User (SU)-MIMO system employing precoding in the UE, RN strategy, and gNodeB. In this sense, to enable the precoding technique, we assumed that the NR-UE and RN protocols have full channel side information knowledge. In this context, the precoding process in the NR-UE can be described by the product between the mmWave RF transmitter, $\mathbf{M}_{ST} \in \mathbb{C}^{N_T^S \times N_T^S}$, and the baseband precoding matrix, $\mathbf{G}_{BB} \in \mathbb{C}^{N_T^S \times N_s}$. We assume that at the NR-UE, the number of transmitter antennas is N_T^S , the number of data symbols is N_s , and the number of FR2 transmitters (FR2-Tx) is the same as the transmitter antennas. Therefore, the transmitted signal from the user equipment can be given by

$$\mathbf{X} = \mathbf{M}_{ST} \mathbf{G}_{BB} \mathbf{S}, \tag{1}$$

where $\mathbf{S} \in \mathbb{C}^{N_s \times T}$ data symbols with T is the number of used subcarriers for the transmission, and power normalization is satisfied such that $\|\mathbf{M}_{ST} \mathbf{G}_{BB}\|_F^2 = TN_T^S$. Figure 2 displays the 3GPP 5G NR uplink system model used to represent the NR-UE in this paper. The input data symbols (N_s) are fed into the UL-SCH and PUSCH coding block and over the resultant PUSCH is applied the modulation scheme (in this paper 64-QAM and 256-QAM have been implemented) and the precoding stages. Then, these complex-valued modulation symbols are mapped onto one or multiple transmission layers on the antenna ports. After that, reference signals are inserted, and therefore, these symbols of each antenna port, including data and reference signals, are modulated into complex-valued time-domain CP-OFDM signals, which be up-converted to an mmWave FR2 band by means of \mathbf{M}_{ST} . It should be noted that the generation and configuration of the signals and channels in the NR-UE fulfill the uplink 5G NR standardization of the 3GPP, which is one of the main novelties of our proposal.

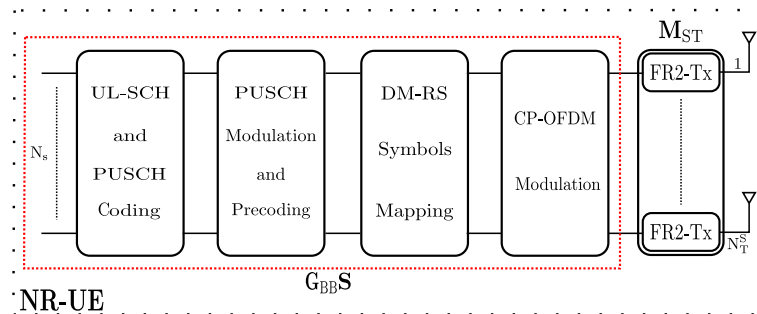


Figure 2. Baseband mmWave NR-UE architecture.

2.1. A&F Signal Model

A single-user uplink mmWave MIMO new radio transmission model for an A&F relay node is introduced in this subsection. The main functionality of this protocol is to capture the mmWave signal from NR-UE and, after that, amplify it and forward it to the gNodeB without performing any additional processing. Additionally, the 3GPP classification can be defined as a Layer 1 (L1) relay node. Therefore, consider the uplink of an SU-mmWave MIMO co-operative system in Figure 1 and the A&F architecture in Figure 3, consisting of an A&F protocol that has N_R^R receiver antennas which correspond with the number of RF mmWave chains (FR2-Rx) and N_T^R represents the FR1 transmitter antennas (FR1-Tx), where we consider that $N_R^R = N_T^R$.

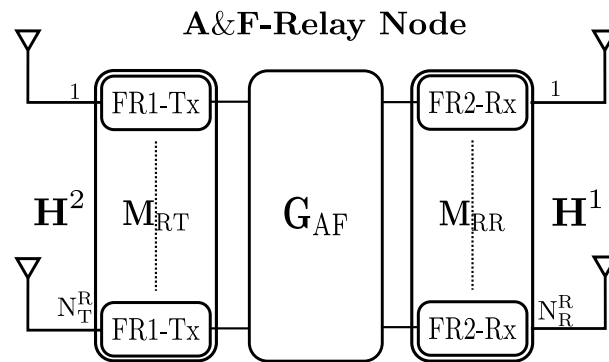


Figure 3. Uplink mmWave MIMO new radio amplify-and-forward relay node architecture.

Let \mathbf{X} denote the symbol matrix to be transmitted by the NR-UE. In the first hop, the received $N_R^R \times T$ -dimensional signal \mathbf{Y}_{AF}^1 at the mmWave MIMO A&F strategy can be expressed as

$$\mathbf{Y}_{AF}^1 = \mathbf{H}^1 \mathbf{X} + \mathbf{N}_{AF}^1, \tag{2}$$

where $\mathbf{H}^1 \in \mathbb{C}^{N_R^R \times N_T^S}$ describes an NR-UE-to-A&F node FR2 (26 GHz) mmWave channel matrix. $\mathbf{N}_{AF}^1 \in \mathbb{C}^{N_R^R \times T}$ denotes Additive White Gaussian Noise (AWGN) matrix with independent and identical distributed random variables $N \sim (0, \sigma_{N_{AF}^1}^2)$, where $\sigma_{N_{AF}^1}^2$ is the noise variance. The signal \mathbf{Y}_{AF}^1 is received through FR2-Rx chains $\mathbf{M}_{RR} \in \mathbb{C}^{N_R^R \times N_R^R}$ in the A&F relaying technology. Nevertheless, it is precoded by precoder matrices $\mathbf{R}_{BBR} \in \mathbb{C}^{N_R^R \times N_R^R}$ and $\mathbf{R}_{BBT} \in \mathbb{C}^{N_R^R \times N_R^R}$, and RF chains $\mathbf{M}_{RT} \in \mathbb{C}^{N_T^S \times N_R^R}$. In addition, the product $\mathbf{R}_{BBT} \mathbf{R}_{BBR} = \mathbf{G}_{AF}$, which depicts a diagonal matrix that on the principal diagonal contains a gain vector (\mathbf{g}_{AF}). Considering the processing described above, the transmit signal at the Uplink A&F RN is written as

$$\mathbf{X}_{AF} = \mathbf{M}_{RT} \mathbf{G}_{AF} \mathbf{M}_{RR}^H \mathbf{Y}_{AF}^1, \tag{3}$$

where \mathbf{M}_{RR}^H denotes the hermitian matrix of \mathbf{M}_{RR} . In the second phase, the received signal at the gNodeB can be given by

$$\mathbf{Y}_{AF}^2 = \mathbf{H}^2 \mathbf{X}_{AF} + \mathbf{N}_{AF}^2, \tag{4}$$

where $\mathbf{H}^2 \in \mathbb{C}^{N_D^D \times N_T^R}$ describes the relay-to-destination channel matrix, and the matrix \mathbf{N}_{AF}^2 represents the components of AWGN, where $\in \mathbb{C}^{N_D^D \times T}$ with $N \sim (0, \sigma_{N_{AF}^2}^2)$. At the destination node, the received signal (4) is processed by the RF matrix $\mathbf{M}_{DR} \in \mathbb{C}^{N_D^D \times N_R^D}$ and baseband matrix $\mathbf{T}_{BB} \in \mathbb{C}^{N_d \times N_R^D}$, which are equivalent to the inverse processing performed by the NR-UE. The received signal is converted to baseband frequency and the baseband signal and physical channels are demodulated and decoded, respectively. Finally, the estimated signal of the destination can be expressed as

$$\begin{aligned} \hat{\mathbf{S}} &= \mathbf{T}_{BB}^H \mathbf{M}_{DR}^H (\mathbf{H}^2 \mathbf{X}_{AF} + \mathbf{N}_{AF}^2) \\ &= \mathbf{T}^H \mathbf{H}^2 \mathbf{M}_{RT} \mathbf{G}_{AF} \mathbf{M}_{RR}^H \mathbf{H}^1 \mathbf{G} \mathbf{S} + \mathbf{N}_D, \\ &= \mathbf{S} + \mathbf{N}_D \end{aligned} \tag{5}$$

where $\mathbf{T} = \mathbf{T}_{BB} \mathbf{M}_{DR}$, $\mathbf{G} = \mathbf{M}_{ST} \mathbf{G}_{BB}$, and $\mathbf{N}_D = \mathbf{T}^H (\mathbf{H}^2 \mathbf{M}_{RT} \mathbf{G}_{AF} \mathbf{M}_{RR}^H \mathbf{N}_{AF}^1 + \mathbf{N}_{AF}^2)$. In (5), the first term is the desired signal and the second term is the noise, which denotes the noise in the backhaul and access links at the co-operative system, respectively.

2.2. D&F Signal Model

In a similar way as in the previous subsection, the transmission model for the proposed uplink mmWave MIMO D&F strategy can be described. A decode-and-forward relay node

is equivalent to a Layer 2 relay taking into account the standardization of the 3GPP, in which the RF signal from NR-UE is first decoded and, before being forwarded to the destination source (gNodeB), it is encoded again. The receiver system model of the protocol is presented, followed by the transmitter model based on the structure described in Figure 4. It is worth highlighting that D&F strategy is performed in two stages: firstly, decoding of the received signal, and, before forwarding the signal to the destination, encoding of the estimated symbols, as shown in Figure 4, which supposes the major difference in comparison with other protocols, such as the amplify-and-forward strategy. It should be noted that, in this paper, two types of uplink D&F relaying protocols have been developed: (a) one with the channel knowledge that performs a Perfect Channel Estimation (PCE) and (b) one that performs a channel estimation through a Least Square (LS) estimator. Additionally, both strategies consider the equalization technique by means of the MMSE algorithm and the protocols are equipped with N_R^R and N_T^R , respectively—receiver and transmitter antennas.

Considering Figure 1 and the transmitted mmWave signal (1) from the NR-UE, in the access link, the received data at the out-band D&F strategy in a block can be expressed as

$$Y_{DF}^1 = H^1 X + N_{DF}^1, \tag{6}$$

where matrix $N_{DF}^1 \in \mathbb{C}^{N_R^R \times T}$ with $N \sim (0, \sigma_{N_{DF}^1}^2)$ describes the AWGN in the first hop, $\sigma_{N_{DF}^1}^2$ is the noise variance. $H^1 \in \mathbb{C}^{N_R^R \times N_T^S}$ denotes the mmWave MIMO channel matrix between the NR-UE and mmWave MIMO D&F RN. In the D&F protocol, the signal (6) is captured through the matrix $M_{RR} \in \mathbb{C}^{N_R^R \times N_R^R}$, as can be seen in Figure 4 and which in the real environment can be emulated by an mmWave RF receiver chains that will be described in Section 3.

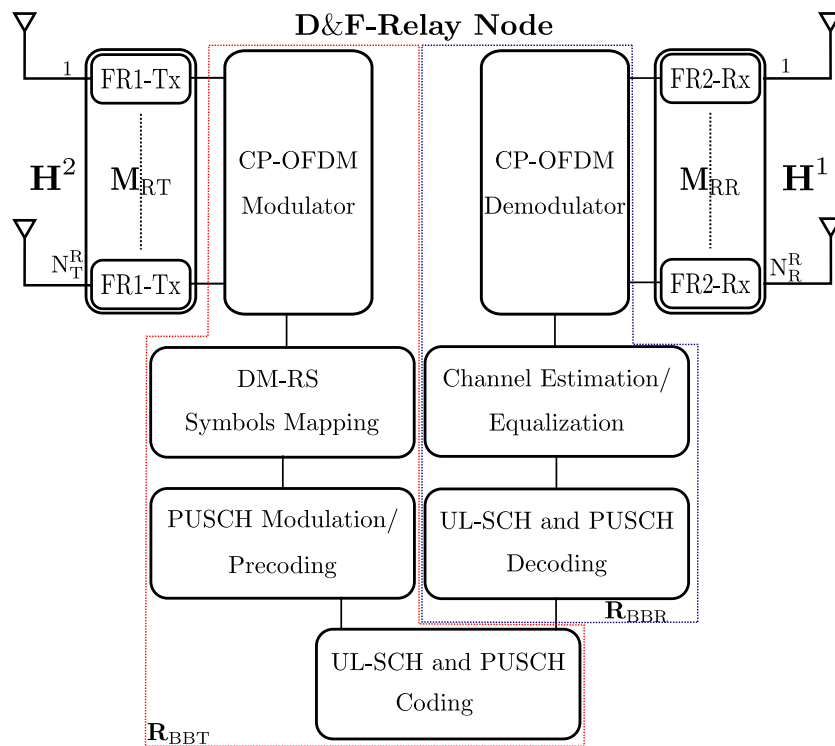


Figure 4. Uplink mmWave MIMO new radio decode-and-forward relay node architecture.

In fact, the decoding and encoding stages are performed by the matrices $R_{BBR} \in \mathbb{C}^{N_s \times N_R^R}$ and $R_{BBT} \in \mathbb{C}^{N_T^R \times N_s}$, respectively. Consequently, the signal transmitted by the RN can be given as

$$\hat{X} = M_{RT} R_{BBT} \tilde{S}, \tag{7}$$

where matrix $\mathbf{M}_{RT} \in \mathbb{C}^{N_T^R \times N_T^R}$ denotes the transmitter < 6 GHz chains of the RN. On the other hand, $\mathbf{R}_{BBT} \in \mathbb{C}^{N_T^R \times N_s}$ is the baseband matrix and $\tilde{\mathbf{S}}$ represents the estimated data symbols matrix at the D&F protocol. Considering (7), the received signal at the gNodeB can be written by

$$\mathbf{Y}_{DF}^2 = \mathbf{H}^2 \hat{\mathbf{X}} + \mathbf{N}_{DF}^2, \tag{8}$$

where $\mathbf{H}^2 \in \mathbb{C}^{N_R^D \times N_T^R}$ is the channel matrix of the backhaul link (D&F-to-gNodeB link) and $\mathbf{N}_{DF}^2 \in \mathbb{C}^{N_R^D \times N_T^R}$ denotes the AWGN with $N \sim (0, \sigma_{N_{DF}^2}^2)$, where $\sigma_{N_{DF}^2}^2$ is the noise variance in the backhaul link. Then, considering the data processing at the gNodeB by means of \mathbf{M}_{DR} and \mathbf{T}_{BB} , where the estimated received signal at the destination can be given as

$$\begin{aligned} \hat{\mathbf{S}} &= \mathbf{T}_{BB}^H \mathbf{M}_{DR}^H (\mathbf{H}^2 \hat{\mathbf{X}} + \mathbf{N}_{DF}^2) \\ &= \mathbf{G}^H \mathbf{H}^2 \mathbf{R}_{RT} \tilde{\mathbf{S}} + \mathbf{N}_D, \\ &= \tilde{\mathbf{S}} + \mathbf{N}_D \end{aligned} \tag{9}$$

where $\mathbf{N}_D = \mathbf{T}^H \mathbf{N}_{DF}^2$, $\mathbf{T} = \mathbf{T}_{BB} \mathbf{M}_{DR}$, and $\mathbf{R}_{RT} = \mathbf{M}_{RT} \mathbf{R}_{BBT}$. In (9), the first term is the desired signal and the second term is the noise, which represents the noise in the backhaul link at the decode-and-forward (D&F) co-operative system, respectively.

2.3. Uplink mmWave MIMO A&F Implementation

In this subsection, we propose the scheme to simulate the uplink mmWave MIMO A&F relay node with a standardized 5G signal by 3GPP. Here, we present an L1 A&F conventional, as shown in Figure 5. In the first phase, the mmWave IQ signal is captured with the mmWave receiver chains (\mathbf{M}_{RR}) through the SimulinkTM software, which will be explained in detail in the next section.

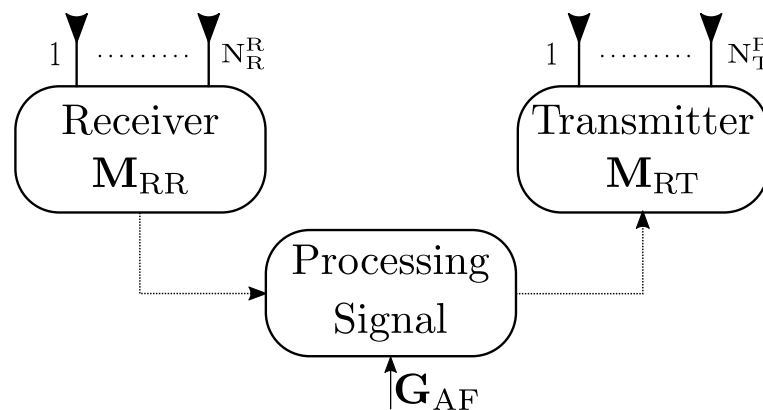


Figure 5. Amplify-and-forward (A&F) uplink mmWave MIMO new radio relay node processing blocks.

After acquiring the received information, the signal is saved in the buffer (processing signal block). Thus, the \mathbf{G}_{AF} of the relay node is applied to the stored signal. Finally, the amplified signal is transmitted to the destination by means of the Transmitter \mathbf{M}_{RT} block, which is simulated as the RF transmit chains of an SDR platform using the SimulinkTM program. It should be noted that this is an easy implementation and cheap to build. However, the main drawback is that with a low Signal-to-Noise Ratio (SNR), the noise and interference are amplified; therefore, its performance deteriorates.

2.4. Uplink mmWave MIMO D&F Implementation

In this subsection, we present the mmWave D&F strategy without and with channel knowledge. Our scheme to develop uplink mmWave MIMO D&F relay nodes uses an uplink 5G NR signal standardized by 3GPP. From the implementation point of view, the protocols have been developed using the 5G communication ToolBox of MatlabTM software.

Additionally, Frequency Division Duplexing (FDD-5G), single and multiple antennas, and out-band operation (access link in mmWave band and backhaul link in sub-6 GHz band) have been considered. As mentioned previously, two D&F strategies are proposed and implemented in this paper, the first of which has the channel knowledge to perform receiving signal decoding and the second of which takes into account the Least Square (LS) channel estimator; therefore, this functionality depends on whether it is activated or not, as can be observed in Figure 6.

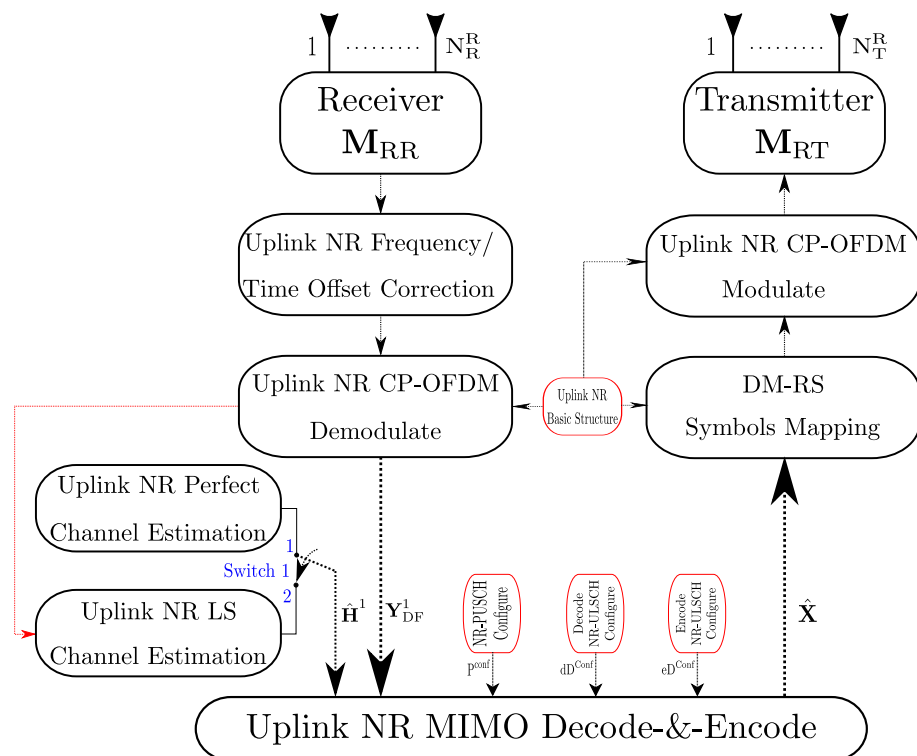


Figure 6. Decode-and-forward (D&F) uplink mmWave MIMO new radio relay node processing blocks.

In Figure 6, the uplink mmWave MIMO new radio decode-and-forward (D&F) relay node processing blocks with and without channel knowledge are presented. From the figure, firstly, IQ signals are captured using the RF mmWave receive chains (M_{RR}), in which the number of receivers antennas is the same to the number of RF mmWave receive (FR2-Rx). After the acquisition of the transmitted data, any significant frequency derivation must be estimated and eliminated, without which many errors would propagate in the uplink received signal. This process is performed correlating the received uplink waveform with the uplink DM-RS. Thus, the adjusted uplink NR received signal is demodulated through the uplink NR CP-OFDM demodulated block. To achieve the signal demodulation, an uplink NR basic structure was used, which supports the sample rate, subcarrier spacing, the number of the Cell Identity (Cell ID), Cyclic Prefix (CP), and the number of Resource Blocks (RBs) of the uplink received waveform. After the steps described above, the algorithm should be determined to obtain the channel matrix, as can be seen in Figure 6. Considering the selected functionality in the relaying protocol, switch 1 will select position 1 (uplink NR perfect channel estimation). In the case of switch point 2, the D&F strategy determines the channel matrix in two stages: (a) the frequency responses for the subcarrier of the pilot symbols are obtained based on the least square algorithm and (b) the frequency responses of the subcarriers of the data symbols can be derived by interpolation methods using the adjacent pilot symbols, as has been employed in [17,18]. The LS estimator is used to

equalize the channel frequency responses at pilot locations sent from different sources at all receiver antennas and can be written as

$$\hat{\mathbf{H}}_P^1 = \mathbf{X}_P^H \mathbf{Y}_{DFP}^1, \quad (10)$$

where $\mathbf{Y}_{DFP}^1 = \mathbf{H}_P^1 \mathbf{X}_P + \mathbf{N}_{DFP}^1$, which is achieved due to the resource blocks in LTE and 5G are allocated over M layers, T subcarriers, and L time slots. Therefore, the matrix \mathbf{Y}_{DF}^1 is comprised of both data symbols and pilot symbols.

Algorithm 1 executes the decoding and encoding of the physical, control, and data channels. In this context, the uplink 5G NR communication system, the Physical Uplink Shared Channel (PUSCH) is used to provide physical layer signaling to support Medium Access Control (MAC) layer operation. From Algorithm 1, it can be observed that the required inputs are the following: the estimated channel ($\hat{\mathbf{H}}^1$), the uplink demodulated received signal (\mathbf{Y}_{DF}^1), the NR-PUSCH, decode NR-ULSCH, and encode NR-ULSCH configure blocks, which provide the parameters to decode and encode the PUSCH and UL-SCH channels. It should be noted that several modulation options can be applied to the PUSCH, including Q-PSK, 16-QAM, 64-QAM, and 256-QAM, where the 64-QAM and 256-QAM modulation schemes have been used in the proposed link-level co-operative simulator demonstrating the flexibility of ours simulator.

Algorithm 1: Uplink MIMO NR decode-and-encode with MMSE algorithm

Input : $\mathbf{Y} = \mathbf{Y}_{DF}^1, \hat{\mathbf{H}} = \hat{\mathbf{H}}^1, P^{conf}, dD^{conf}, eD^{conf}$
Output: $\hat{\mathbf{X}}$
 $[N_{sub}, N_{sym}, N_T^S, N_R^R] = \text{size}(\mathbf{Y}_{DF}^1);$
if $N_T^S == 1 \ \&\& \ N_R^R == 1$ **then**
 $\hat{\mathbf{Y}} = (\hat{\mathbf{H}}^H \hat{\mathbf{H}} + \hat{\mathbf{N}}_0)^{-1} \hat{\mathbf{H}}^H \mathbf{Y};$
else
 for $c \leftarrow 1 : N_{sub}$ **do**
 for $s \leftarrow 1 : N_{sym}$ **do**
 $\hat{\mathbf{Y}}_{(c,s)}^{(\cdot)} = \frac{(\hat{\mathbf{H}}_{(c,s)}^{H(\cdot)} \hat{\mathbf{H}}_{(c,s)}^{(\cdot)} + \hat{\mathbf{N}}_0 \mathbf{I})^{-1} \hat{\mathbf{H}}_{(c,s)}^{H(\cdot)} \mathbf{Y}_{(c,s)}^{(\cdot)}}{\mathbf{I}};$
 for $i \leftarrow 0 : N_{sl}$ **do**
 $[\text{ulsch}^b, \text{pusch}^s] = \text{NR-PUSCH}^d(\hat{\mathbf{Y}}^i, \hat{\mathbf{H}}^i, P^{conf});$
 $[\text{data}^b] = \text{NR-ULSCH}^d(\text{ulsch}^b, \text{pusch}^s, P^{conf}, dD^{conf});$
 $[\text{ulsch}_{tx}^b] = \text{NR-ULSCH}^c(\text{data}^b, P^{conf}, eD^{conf});$
 $[\text{pusch}_{tx}^s] = \text{NR-PUSCH}^c(\text{ulsch}_{tx}^b, P^{conf});$
 $[\hat{\mathbf{x}}] = \text{NR-P}^c(\text{pusch}_{tx}^s);$
 $[\hat{\mathbf{X}}] = \text{Cat}(\hat{\mathbf{X}}, \hat{\mathbf{x}});$

On the other hand, in order to maximize the SNR, the Mean Maximum Square Error (MMSE) equalizer has been considered, which employs the $\mathbf{Y}_{DF}^1, \hat{\mathbf{H}}^1$, and estimated noise for its implementation. Furthermore, in the proposed algorithm, the subindices $(\cdot)^d$ and $(\cdot)^c$ in the functions describe the processes of decoding and encoding, as well as the subindices $(\cdot)^b$ and $(\cdot)^s$ in the outputs of the functions represent data bits and data symbols, respectively. The NR-P^c function, mapping each symbol, in the resource grid, and the $\hat{\mathbf{x}}$ subframe to the output of the function, is obtained. Finally, concatenating of each subframe is performed by means of the $\text{Cat}(\cdot)$ function, from which all frames to be re-transmitted are stored. After that, $\hat{\mathbf{X}}$ is processed through the DM-RS symbols mapping block, where reference signals are added to the resource grid. The resultant signal to the output of blocks is modulated considering the uplink NR CP-OFDM modulate block. Then, the resultant waveform is passed by the FR1-Tx transmitter \mathbf{M}_{RT} block, which performs the translation

in frequency of baseband to the FR1 band and transmits the signal to gNodeB, as has been seen in Figure 6.

3. Link-Level Co-Operative Simulator

In this section, the link-level co-operative simulator for the uplink mmWave MIMO NR relay node co-operative system is described and presented in Figure 7. To achieve its simulation, the Matlab™ and Simulink™ software have been used. Furthermore, it should be noted that the developed link-level co-operative simulator takes into account realistic assumptions for node implementations, for example, NI-USRP 2944R, mmWave Transmitter Chain, and mmWave Receiver Chain, in which the two last will be described in detail in this section. From the figure, it can be seen that the developed simulator is composed of one New Radio User Equipment (NR-UE), which is achieved with a baseband unit through the Matlab™ tool, where the digital algorithms, for example, symbol generation, M-QAM modulation scheme, coding of the UL-SCH and PUSCH channels, and CP-OFDM waveform generation, have been performed. These characteristics fulfill the requirements of the 5G uplink 3GPP in [19,20]. Additionally, the RF stage (Digital/IF/RF Unit) is implemented by means of Simulink™ software, where the mmWave Transmitter architecture has been developed [18] and is shown in this section.

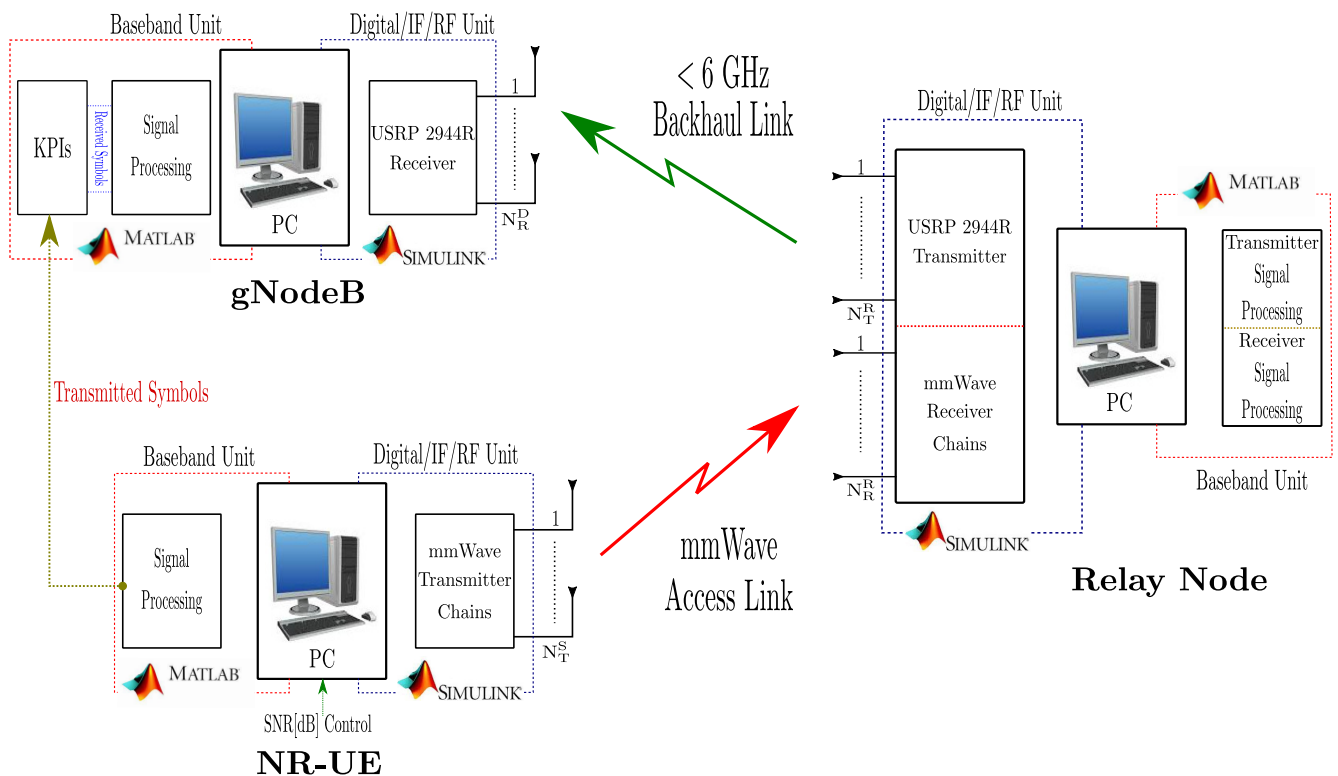


Figure 7. Architecture of the link-level co-operative simulator for uplink mmWave MIMO NR relay node system.

At present, there are many computer programs that simulate the real operation of communications systems, especially when their implementation is mathematically complex or difficult to reproduce. In this sense, in this work the Matlab™ and Simulink™ software are used, also employing the Monte-Carlo simulation method. Here, the Monte-Carlo method, considering the simulator in Figure 7, first determines and configures the input signals. Therefore, the frame number (10^3) to evaluate has been defined for each SNR point, as well as the SNR vector, which in this work has been defined from 0 to 20 dB with a step of 2 dB. After that, the transmitted data symbols are randomly generated in the NR-UE. Additionally, the PUSCH and UL-SCH encoders are configured taking into account the transmitted data symbols and the employed modulation scheme (64-QAM

and 256-QAM). The other determined input parameters are the configurator of the access link channel in the mmWave band (26 GHz) and the backhaul link channel in the 3.5 GHz band. Furthermore, the path loss in the access and backhaul links are calculated taking into account the expression described in this section. On the other hand, the encoding and decoding functions in the NR relay node are defined. In the gNodeB side, the decoding functions are configured with the arrays to store the Key Performance Indicators (KPIs) of the system, and in this paper the throughput and Bit Error Rate (BER) have been measured. By creating the input variables, we are prepared to simulate the processing loop in the Monte-Carlo method, which is described by Algorithm 2.

Algorithm 2: Monte-Carlo processing loop in the link-level co-operative simulator

```

for  $i \leftarrow 1 : 2 : SNR$  do
  for  $j \leftarrow 1 : Frame$  do
    1. Transmitted data symbols from NR-UE.
    2. Transmitted signal passes through the mmWave channel and it is
       added the path loss in the Access Link.
    3. mmWave signal is captured, processed, and transmitted by
       the NR Relay Node (A&F or D&F).
    4. Transmitted signal by the RN passes by means of backhaul channel
       and, furthermore it is summed the path loss of the link.
    5. Calculates and stores the metric of the throughput for each frame.
    6. Determines and store the BER for each frame, considering
       the transmitted signal by the NR-UE.
  Calculates and stores the throughput mean for each SNR point.
Determines and stores the BER mean for each SNR point.

```

On the other hand, A&F, D&F with or without the knowledge channel relaying protocols were carried out through MatlabTM (for the baseband signal processing) and SimulinkTM (for the RF stage) software. In Figure 7, the relay node shows two blocks, respectively, inside the digital/IF/RF unit and baseband unit, which describe the receiver and transmitter stages in the relaying protocol. For the first stage of the NR-relay node, an mmWave receiver chain has been designed and implemented by means of SimulinkTM.

Now, the functionality of the baseband unit of the relay node depends on the used relaying protocol, as well as was described in Section 2. In this context, the baseband unit in the A&F relay node amplifies the received signal and is transmitted to the gNodeB through the digital/IF/RF unit transmitter which is emulated as an NI-USRP 2944R. However, when the D&F relay node with or without the knowledge channel is considered, the receiver signal processing and transmitter signal processing stages are performed, respectively—demodulation-decoding and encoding-modulation algorithms. After that, the modulated signal is transmitted by means of the NI-USRP 2944R transmitter RF stage to destination (gNodeB). The last node in our link-level co-operative simulator is the gNodeB, which is achieved through an RF stage in SimulinkTM (simulated with the same characteristics of a NI-USRP 2944R) and a baseband unit developed by MatlabTM tool, where the received signal decoding has been performed. Additionally, as can be seen in Figure 7, the transmitted symbols by the NR-UE node is determined and compared with the detected symbols in baseband units in the gNodeB. In this sense, the Key Performance Indicators (KPIs) of the bit error rate (BER) and throughput of the uplink mmWave MIMO NR relay node co-operative system have been measured.

3.1. Network Model: Topology and Communication Channel

In this subsection, the description of the scenario and the channel models used in the link-level co-operative simulator will be introduced. The simulation scenario to the assessment of uplink mmWave MIMO NR-relay node co-operative network through the proposed link-level co-operative simulator is presented and described. A series of Monte-Carlo simulations in an urban environment, particularly in the indoor-to-outdoor scenario has been performed. Thus, the indoor-to-outdoor environment scenario with uplink mmWave MIMO new radio relay protocol, which has been considered in this paper, is presented in Figure 8. Hence, there is a line-of-sight channel in both links, between the NR-UE and NR-relay node and the NR-relay node and gNodeB, respectively. The 5G network in Figure 8 is composed of one NR-UE, which serves an uplink gNodeB by means of the mmWave new radio relay node (NR RN). As seen from the figure, A&F and D&F mmWave new radio RNs have been designed, where the protocols operate in out-band frequency. Therefore, the access link and backhaul link work, respectively, at 26 GHz, taking advantage of the unlicensed bands (FR2) and in sub-6 GHz bands in accordance with 5G standards (FR1), as has been described in the previous section. The relays used in the mmWave two-hop architecture are out-band and are intended to extend the 5G mobile coverage to an indoor environment. In the topology, the NR-relay node can use either the A&F and D&F relaying strategies. Finally, the direct link between the NR-UE inside the building and the gNodeB have not been simulated due to both nodes work in the different frequency bands and, additionally, the 5G base station coverage is unreachable by the NR-UE. In the developed link-level co-operative simulator, the performance of both proposed and implemented relays will be compared to observe the improvement achieved by our mmWave architecture.

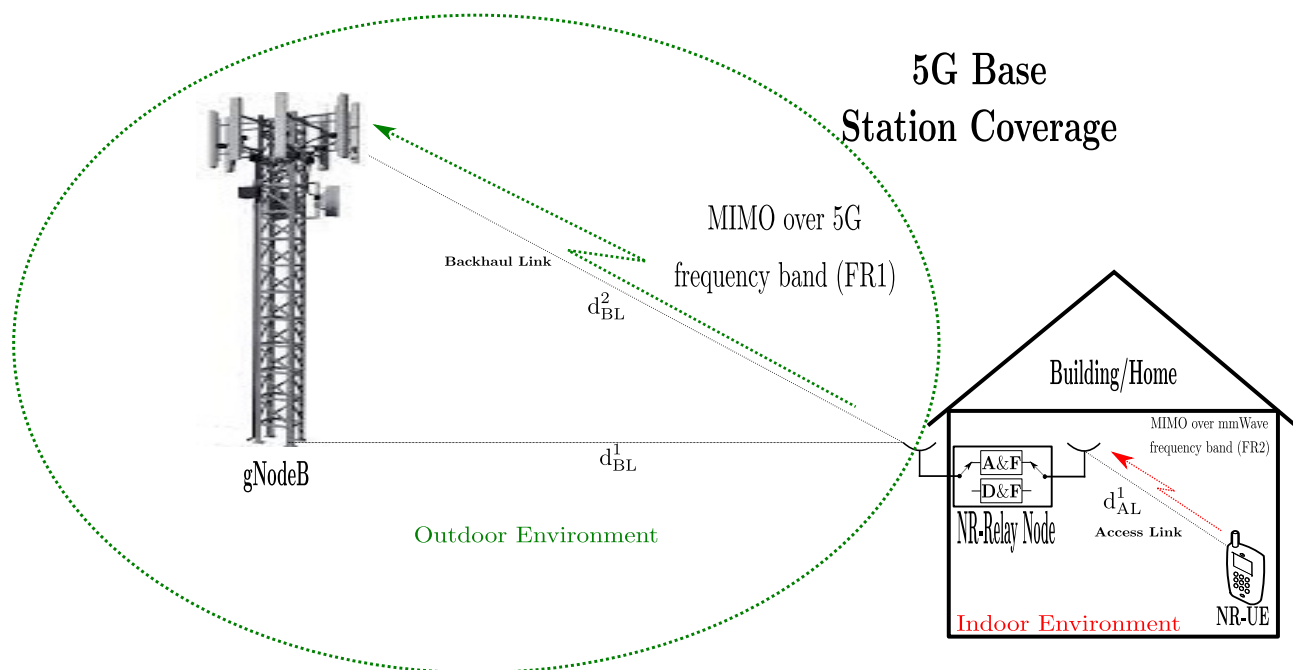


Figure 8. Indoor-to-outdoor environment scenario with uplink mmWave MIMO new radio relay protocol.

In Table 1, the corresponding distances to determine the path loss of the indoor-to-outdoor environment proposed and simulated in this paper are presented.

Table 1. Distance of the simulation scenario.

Parameters	Values
h_{gN}	25 m
h_{RN}	19.5 m
d_{BL}^1	67 m
d_{BL}^2	67.3 m
d_{AL}^1	6.88 m

Then, the channel and path loss models used in the link-level co-operative simulator will be explained in detail. It should be highlighted that the employed channel model is emulated through MatlabTM ToolBox software, which considers standardization of the 3GPP [21]. In this work, we have assumed that the access link is implemented as a Line-of-Sight (LOS) channel, and the channel model of the Clustered Delay Line (CDL)-D [22] were considered. It should be noted that, in [22], a large number of 5G NR propagation channels show support frequency bands over the range 0.5–100 GHz, which can simulate environments such as an urban microcell street canyon, urban macrocell, indoor office, rural macrocell, and mobility, also including, a geometry-based stochastic channel model. In this sense, the 3GPP indoor office path loss model is used to emulate the mmWave LOS channel access link, being capable of simulating various typical indoor deployments. Accordingly, the mmWave indoor office path loss model can be written by

$$PL_{AL} = 32.4 + 17.3 \log_{10}(d_{AL}^1) + 20 \log_{10}(f_c) + \sigma_{AL} \quad 1 \text{ m} \leq d_{AL}^1 \leq 100 \text{ m}, \quad (11)$$

where d_{AL}^1 (m) represents the distance between NR-UE and NR-RN and σ_{AL} denotes the shadowing term with zero mean and standard deviation of 3 dB. Additionally, f_c is the carrier frequency in GHz. On the other hand, the CDL-D channel model is considered for the FR1 backhaul link, which is modeled according to the specification of the 3GPP and emulated by the communication ToolBox of MatlabTM software. The 3GPP Urban Macrocell (Uma) path loss model is employed to represent the outdoor sub-6 GHz LOS bckhaul link; therefore, the expressions can be given by

$$PL_{BL}(\text{dB}) = \begin{cases} PL_1 + \sigma_{BL} & 10 \text{ m} \leq d_{BL}^1 \leq d_{BL}^+ \\ PL_2 + \sigma_{BL} & d_{BL}^+ \leq d_{BL}^1 \leq 5 \text{ km} \end{cases} \quad (12)$$

where d_{BL}^1 (m) is the distance from NR-RN to the gNodeB, as shown in Figure 8. Besides, d_{BL}^+ (m) is the breakpoint distance, which can be obtained as in [22], besides, PL_1 (dB) and PL_2 (dB) are the path losses that can be given by

$$PL_1(\text{dB}) = 28.0 + 22 \log_{10}(d_{BL}^2) + 20 \log_{10}(f_c), \quad (13)$$

and

$$PL_2(\text{dB}) = 28.0 + 40 \log_{10}(d_{BL}^2) + 20 \log_{10}(f_c) - 9 \log_{10}((d_{BL}^+)^2 + (h_{RN} - h_{gN})^2), \quad (14)$$

where d_{BL}^2 (m) is the distance from the NR-RN antennas to the gNodeB antennas and h_{gN} and h_{RN} are the heights of the gNodeB and NR-RN in (m), respectively. σ_{BL} represents the shadowing term with zero mean and a standard deviation of 6 dB, and f_c is the carrier frequency in GHz.

3.2. Description of the Transmitter (Tx) and Receiver (Rx) mmWave Chains

The mmWave radio transmitter chain in Figure 9 translates the signal from baseband frequency to FR2 band (26 GHz), after the application of the baseband algorithms to the transmitted data symbols at the NR-UE. The signal in the mmWave frequency band will be transmitted through the radio channel and the received signal will be converted, through

the mmWave radio receiver (FR2-Rx), into a baseband digital signal at the relay node. This architecture was developed based on that described in [18], and for its implementation we used off-the-shelf subsystems.

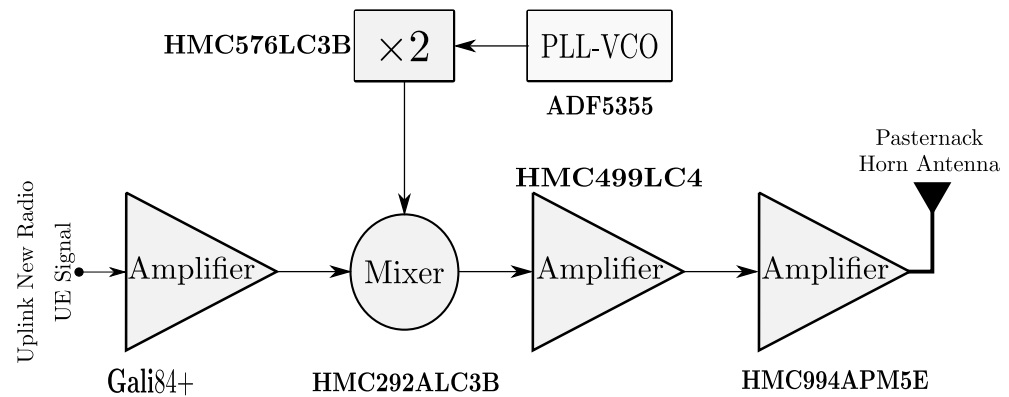


Figure 9. Implementation architecture of the mmWave transmitter chain (FR2-Tx).

The uplink 5G waveform signal was applied to the input of a Mini-Circuits Gali84+ Amplifier [23], which was placed before the Hittite HMC292ALC3B mixer [24]. To achieve Local Oscillator (LO) signals, we employed an Analog Devices ADF5355 Phase-Locked Loop (PLL) [25] and Hittite HMC576LC3B [26] frequency doubler. We highlight that the PLL-VCO integrated a wideband microwave VCO design, which allows frequency operation from 6.8 to 13.6 GHz at one radio frequency output. After using the mixer, Hittite HMC499LC4 [27] and Hittite HMC944APM5E [28], respectively, and an mmWave medium power amplifier and power amplifier were used. The last subsystem in Figure 9 is the Pasternack PE9821/2FWR-24 [29] waveguide horn antenna with 20 dB gain, which was employed at the output of the mmWave transmitter chain. In Figure 10, its block architecture can be observed, which has the same structure as the mmWave transmitter chain presented previously and employs equivalent components, except that power amplifier has been replaced by a Low Noise Amplifier (LNA), Hittite HMC519LC4 [30]. It should be noted that the signal in the mmWave frequency band (26 GHz) transmitted by the NR-UE through the radio channel is received by the mmWave receiver chain in Figure 7 and will be converted into a baseband digital signal at the baseband stage in the relay node strategy.

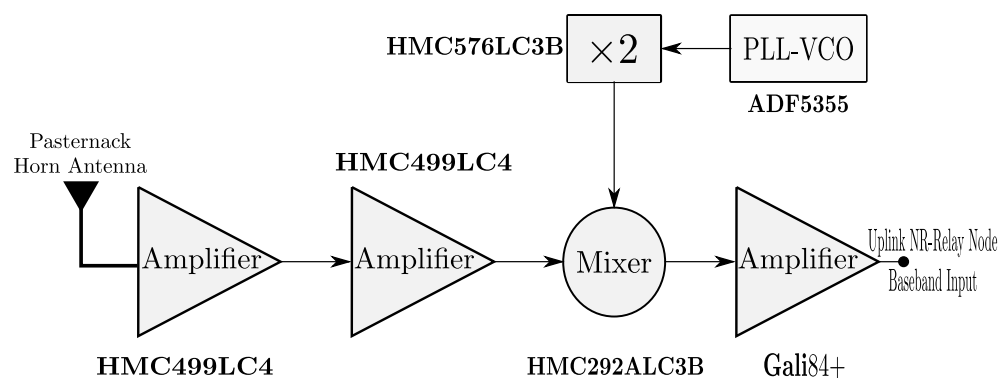


Figure 10. Implementation architecture of the mmWave receiver chain (FR2-Rx).

As mentioned above, the simulator was designed with interconnection of off-the-shelf components, allowing for easy characterization and integration into the transceiver (Rx-Tx) mmWave radio link-level co-operative simulator. The electrical specifications of the different RF subsystems are described in Table 2.

Table 2. Parameters of the elements of mmWave transmitter and receiver chains.

Parameters	Gali ₈₄	HMC292ALC3B	HMC499LC4	HMC944APM5E	HMC519LC4
Frequency Range (GHz)	0 to 6	14 to 30	24 to 28	20 to 28	18 to 28
G_{lin} (dB)	19.2	−9	16	16	14.4
Local Oscillator Freq. (GHz)	-	25	-	-	-
Input Return Loss (dB)	18	13.2	8	12	15
Output Return Loss (dB)	8.9	12.5	12	22	20
OIP3 (dBm)	38	20	34	36	23
$P_{1\text{dB,out}}$ (dBm)	21.2	9	23	27	11
$P_{\text{sat,out}}$ (dBm)	22.1	13	23.5	28	14
Noise Figure (dB)	4.4	10	5	4	3.5
GS_{sat} (dB)	3.5	2.2	4	5	6

4. Simulation Results and Discussion

The obtained results from the simulator are explained in this section. Therefore, to evaluate the validity of the two-hop uplink mmWave MIMO RN co-operative network through the proposed link-level co-operative simulator described in this paper, Monte-Carlo simulations are performed for each signal-to-noise ratio (SNR) transmission and 10^3 frames, where the relaying protocols process the uplink received signal and forward it to the destination. Link-level simulations are generally used to simulate end-to-end physical layer technologies, where there is one base station, and consider an accurate scenario model to emulate channels and propagation losses. Furthermore, in each iteration, independent sets of channel realizations and noise are used. For the simulations, only one gNodeB, one new radio relay node, and one NR-UE are considered. In the section, the key performance indicators (KPIs), bit error rate (BER) and throughput versus SNR of the proposed two-hop uplink relay co-operative system, have been assessed. We consider a network encompassing one NR-UE equipped with $N_T^S = \{1, 2\}$ transmitter antennas, and transmitting 64-QAM and 256-QAM modulation schemes. The RN (A&F or D&F) is equipped with $N_R^R = N_T^R = \{1, 2, 4\}$ receiver and transmitter antennas. Additionally, the gNodeB is carried out using $N_R^D = \{1, 2, 4\}$ receiver antennas. Note that, when performing MIMO simulations, you will have as many transmitter and receiver chains as the number of antennas used in the simulation. This process is then repeated iteratively, as described above, to obtain more accurate results. In Table 3, the simulation parameters are summarized. Two types of NR co-operative relay nodes are considered: A&F and D&F. In the case of the NR D&F relay node, two situations are developed: (a) an exact knowledge of the channel (PCE) is available and (b) an estimation (LS) of it is made. Furthermore, we have denoted $N_T^S \times N_R^R = N_T^R \times N_R^D$, like the considered MIMO scheme in our uplink mmWave co-operative network.

Table 3. Main parameters of simulation.

Parameters	Backhaul Link	Access Link
Signal Bandwidth	25 MHz	25 MHz
Carrier Frequency	3.5 GHz	26.1 GHz
Tx/Rx schemes	SISO, $2 \times 2 \times 2$ and $2 \times 4 \times 4$	SISO, $2 \times 2 \times 2$ and $2 \times 4 \times 4$
Subcarrier Spacing	30 kHz	30 kHz
Modulations	64-QAM and 256-QAM	64-QAM and 256-QAM
Channel Models	CDL-D	CDL-D
Light-Vision	LOS	LOS

4.1. Bit Error Rate Performance

In this simulation, the objective function studied in this subsection is the bit error rate (BER) between the source (NR-UE) and destination (gNodeB) through the uplink mmWave relay node. Therefore, we compared the overall performance of the implemented relaying algorithms. Figure 11 shows the BER performance comparison of the uplink mmWave

MIMO co-operative network of the NR RNs versus SNR, where the 64-QAM modulation scheme has been considered. Through the comparison of simulation curves, it can be clearly seen that the BER performance of the proposed uplink mmWave SISO A&F protocol is discrete; however, the SISO D&F strategies with PCE and LS algorithms are better than the SISO A&F. Additionally, the uplink mmWave SISO NR-D&F strategy together with PCE exhibited the best performance among the proposed uplink mmWave SISO NR-RNs. In particular, it can be verified that the SISO D&F with PCE reached the BER level of 1.6×10^{-2} at around SNR = 20 dB. In addition, Figure 11 also shows that although the BER performance of the proposed SISO D&F protocol with LS algorithm is less than the SISO D&F with PCE, in this sense, the BER level is 1.9×10^{-2} at 20 dB.

In order to better the performance in the communication between the NR-UE and gNodeB, the MIMO technique has been implemented in the link-level co-operative simulator, with exactly (2×2) or (2×4) mmWave MIMO channels and (2×2) or (4×4) sub-6 GHz MIMO channels in the access link and backhaul link, respectively, were considered. Since our proposed MIMO algorithm, it can be seen that the mmWave co-operative system considerably improved the BER performance, in comparison with the uplink mmWave SISO NR relay node co-operative network. It is interesting to observe that the uplink mmWave $(2 \times 2 \times 2)$ NR-A&F protocol exhibits the same BER level of the SISO D&F with the PCE algorithm at around SNR = 18 dB; therefore, a performance gain of 2 dB is reached.

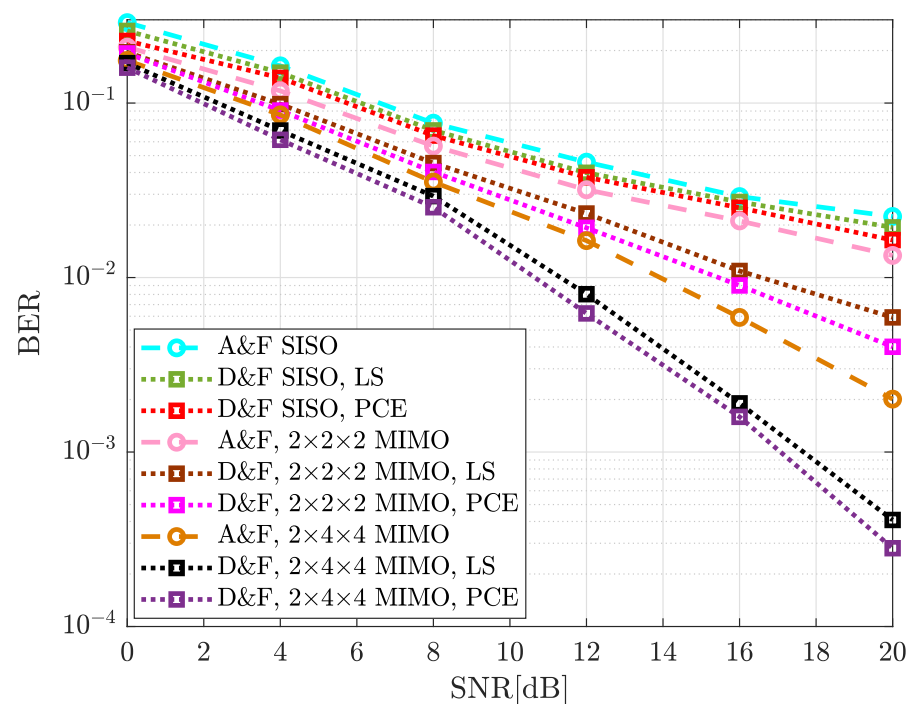


Figure 11. BER comparison for different uplink mmWave NR-RN co-operative schemes implemented with the 64-QAM signal.

As shown in Figure 11, the BER performance of the $(2 \times 4 \times 4)$ MIMO NR-A&F strategy decreases tremendously, which, compared with the $(2 \times 2 \times 2)$ MIMO NR-A&F protocol, is an enhancement of 7.5 dB. In addition, the uplink mmWave MIMO D&F strategies have generated an improved performance. In this context, it can be seen that the $(2 \times 2 \times 2)$ NR-D&F strategy with the LS algorithm reached a BER level of 5.9×10^{-3} at around SNR = 20 dB, which implies that 7.0 dB and 6.0 dB performance gains were successfully achieved, respectively, when compared with SISO NR-D&F and $(2 \times 2 \times 2)$ NR-A&F protocols. However, the obtained result with an uplink mmWave $(2 \times 4 \times 4)$ D&F relay node with the PCE algorithm overcame the relaying scheme described above. For example, it can be seen in Figure 11 that this algorithm generally exhibited a better

BER performance of the proposed strategies and, more specifically, obtained 12 dB of BER gain when compared with the SISO D&F PCE algorithm and 5 dB considering the $(2 \times 4 \times 4)$ A&F strategy. Nevertheless, when the $(2 \times 4 \times 4)$ D&F LS technique was considered, a loss of approximately 0.9 dB was achieved in comparison with the $(2 \times 4 \times 4)$ D&F PCE protocol. Therefore, it should be noted that the practical estimation is very close to the perfect estimation.

Figure 12 illustrates the achievable BER performance of the proposed uplink mmWave NR-RNs, in which the 256-QAM modulation scheme is taken into consideration. It is indicated from Figure 12 that the implemented uplink mmWave MIMO NR-RN co-operative network achieves a lower BER level than the proposed protocols with the SISO technique. More explicitly, the error of the $(2 \times 2 \times 2)$ A&F protocol decreases, the BER level of this scheme improves and approaches the 2.5×10^{-2} BER level at around SNR = 20, which suggests a gain of the 3 dB of the uplink mmWave SISO A&F algorithm. Additionally, when the number of antennas increases, i.e., $(2 \times 4 \times 4)$ configuration, the BER behaviour may reach values of the $(2 \times 2 \times 2)$ D&F PCE performance. On the other hand, when the uplink mmWave $(2 \times 2 \times 2)$ D&F PCE strategy was considered, a 5 dB performance gain was attained and overcame, with SNR = 15 dB, the $(2 \times 2 \times 2)$ A&F protocol. Furthermore, the results clearly show that the uplink mmWave $(2 \times 4 \times 4)$ NR-D&F PCE strategy has the best BER performance among the proposed schemes. In this sense, the same performance as the $(2 \times 4 \times 4)$ A&F protocol has been obtained at SNR = 13.5 dB, such that a 6.5 dB performance gain was achieved. However, it should be noted that the BER performance of the 64-QAM is lower than 256-QAM, which was due to the robustness that changes the 64-QAM modulation scheme to 256-QAM.

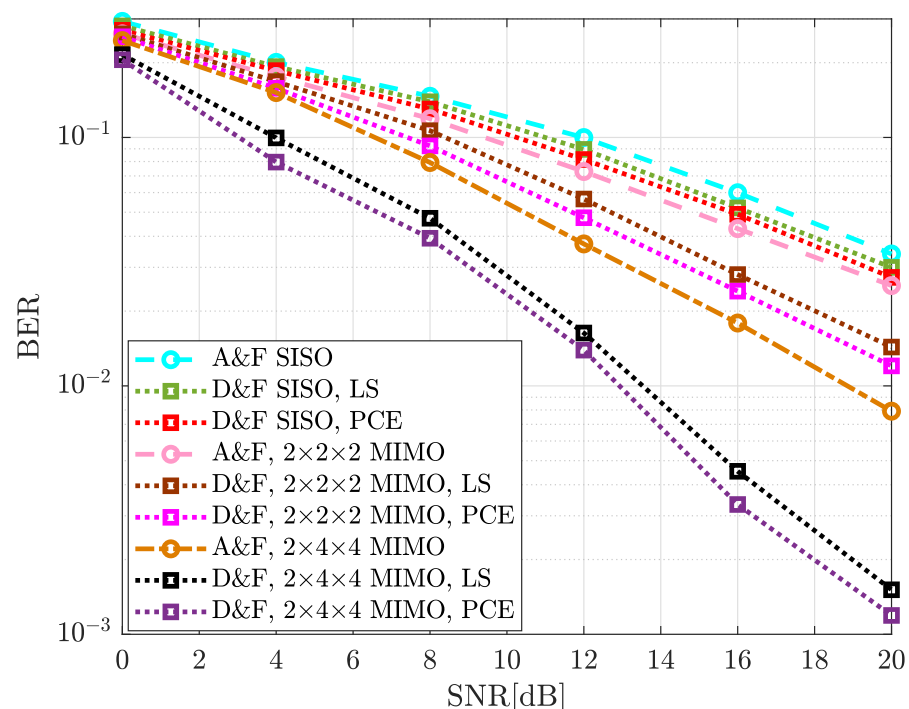


Figure 12. BER comparison for different uplink mmWave NR-RN co-operative schemes implemented with the 256-QAM signal.

4.2. Average Throughput

In this subsection, we examine the achievable capacity performance of the proposed uplink mmWave NR-RNs protocols with single and multiple antennas for the 64-QAM and 256-QAM modulation schemes. It should be highlighted that the number of mmWave RF chains employed in the mmWave co-operative system is the same as the number of antennas, as has been considered in the discussed results in the previous subsection.

The illustrated performance in Figures 13 and 14 describe the output throughput of the new radio UL-SCH transport channel processing. Therefore, Figures 13 and 14 plot the achievable throughput comparison for different proposed uplink mmWave NR-RN co-operative protocols, respectively, with 64-QAM and 256-QAM modulation schemes.

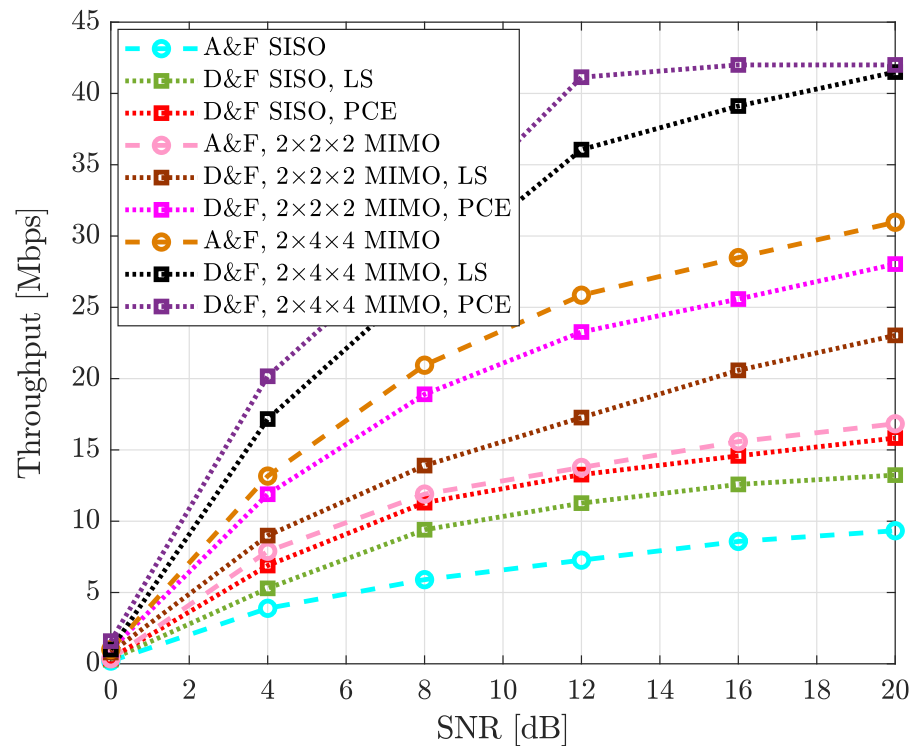


Figure 13. Throughput comparison for different uplink mmWave NR-RN co-operative schemes implemented with the 64-QAM signal.

Figure 13 shows that the achievable capacity performance recorded for the uplink mmWave MIMO NR-RNs reached a higher average throughput than the SISO technique and it can be observed that, by increasing the antenna number the network, greatly improves the throughput system. It can be seen from the figure that the uplink mmWave SISO D&F PCE algorithm achieved approximately the same average throughput as the uplink mmWave (2 × 2 × 2) A&F protocol. Nevertheless, when the SISO D&F LS algorithm is considered, the average performance of the system is low in comparison with the SISO D&F PCE algorithm, for example, the reached maximum throughput was 13.23 Mbps, which was achieved by the uplink mmWave (2 × 2 × 2) A&F and uplink mmWave SISO D&F PCE algorithms, respectively, from 11.4 and 12 dB of the SNR. In Figure 13, it is indicated that the throughput at SNR = 20 dB for (2 × 2 × 2) D&F LS protocol was approximately 23.03 Mbps; however, with channel knowledge, a capacity of 28.05 Mbps could be reached with the same SNR value, which represents a performance gain of about 5 Mbps. On the other hand, when it is compared with an uplink mmWave (2 × 4 × 4) A&F relay node, it was overcome by approximately 8 Mbps. Finally, it should be noted that the maximum throughput of our uplink 5G NR for the 64-QAM modulation scheme is 42 Mbps; in Figure 13, it can be seen that this was reached by the uplink mmWave (2 × 4 × 4) D&F PCE protocol from SNR = 16 dB. Additionally, when the (2 × 4 × 4) D&F LS algorithm was employed, the achieved maximum performance was 41.50 Mbps at SNR = 20 dB, which represents a 0.5 Mbps lower than the reached by the (2 × 4 × 4) D&F PCE protocol.

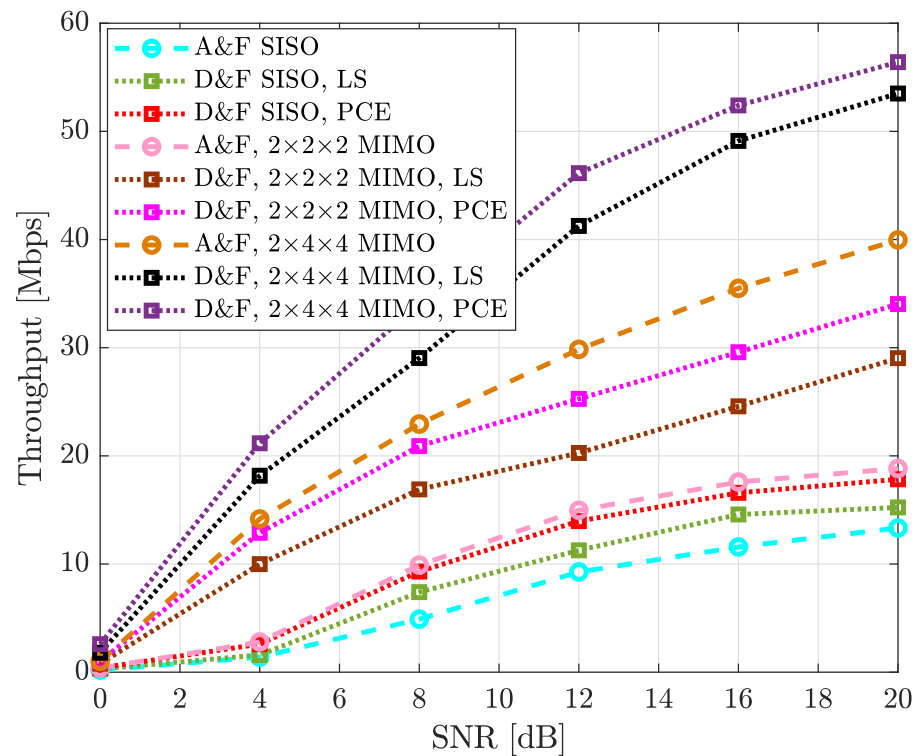


Figure 14. Throughput comparison for different uplink mmWave NR-RN co-operative schemes implemented with the 256-QAM signal.

Here, the simulation results of the proposed uplink mmWave NR-RN co-operative network are given for 256-QAM constellation scheme over the mmWave SISO and MIMO channels. It can be seen in Figure 14 that the uplink mmWave SISO A&F protocol reached a capacity of 13.33 Mbps at around SNR = 20 dB, while with the $(2 \times 2 \times 2)$ antenna scheme, the co-operative network reached the same average throughput at around SNR = 10.2 dB; therefore, a performance gain may be achieved. Moreover, when we further increased the antenna number to the $(2 \times 4 \times 4)$ configuration, the uplink mmWave co-operative network reached 39.97 Mbps at around SNR = 20 dB, implying that a 16.2 dB performance gain was successfully achieved compared to the throughput of the SISO A&F protocol. The achievable performances of uplink mmWave D&F strategies are also depicted in Figure 14. It was observed that the average capacity performance may be improved by the uplink mmWave D&F strategies, which was attained due to the impact of decoding and encoding stages the uplink mmWave received signal was subjected to before being re-transmitted to the gNodeB by means of the uplink mmWave D&F protocols. Furthermore, in the case of the SISO technique, the average capacity of the uplink mmWave D&F PCE protocol at SNR = 20 dB was approximately 17.83 Mbps, where a throughput gain of about 4.5 Mbps was achieved in comparison with the uplink mmWave SISO A&F algorithm. Moreover, when the $(2 \times 2 \times 2)$ antenna configuration was considered in each implemented algorithm, a 34.03 Mbps may be achieved at the SNR = 20 dB by the uplink mmWave D&F PCE protocol, which is associated with performance gains of 12.5 and 4.2 dB, respectively, respect to the uplink mmWave A&F and uplink mmWave D&F LS protocols. Additionally, it should be highlighted that the throughput maximum that could be obtained without any channel for the 5G NR-PUSCH 256-QAM system is 56.4 Mbps, which alone was achieved by the uplink mmWave $(2 \times 4 \times 4)$ D&F PCE protocol at SNR = 20 dB. Nevertheless, when an uplink mmWave $(2 \times 4 \times 4)$ D&F LS strategy was taken into account, the achievable throughput was near to the throughput maximum, approximately 53.5 Mbps, which had a loss of 2.9 Mbps; however, with respect to the uplink mmWave $(2 \times 4 \times 4)$ A&F protocol, a loss 16.46 Mbps was reached.

4.3. Comparative Discussion

In this subsection, to address the complexity of the proposed millimeter band NR-relay nodes, hardware implementation and the arithmetic operations they perform are considered. Firstly, taking into account the development hardware approach, all the proposed relay node technologies are designed considering the same elements, which were explained in the previous sections. However, Table 4 summarizes the required arithmetic operations of the proposed relaying technologies, considering the step of capture, processing, and forwarding of the received signal to the gNodeB.

Table 4. Arithmetic operations required by proposed relay node techniques.

RN Protocols	Products	Summations	Flops
A&F	$N_T^R N_R^R T$	$N_T^R T (N_R^R - 1)$	$2N_T^R N_R^R T - N_T^R T$
D&F, PCE	$N_T^S N_R^R [\frac{7T^3+9T^2-4T}{6}]$ $+T[N_s N_R^R + N_T^R (N_s + N_R^R)]$	$N_T^S N_R^R [\frac{7T^3+15T^2+2T}{6}]$ $+T[N_s (N_R^R - 1) + N_T^R (N_s + N_R^R - 2)]$	$N_T^S N_R^R [\frac{7T^3+12T^2-T}{3}]$ $+T[N_s (2N_R^R + 2N_T^R - 1) + N_R^R (N_T^R + 1) - 2N_T^R]$
D&F, LS	$N_T^S N_R^R [\frac{\lambda\alpha(\alpha+1)}{2} + 20\mu$ $+ \frac{7T^3+9T^2-4T}{6}]$ $+T[N_s N_R^R + N_T^R (N_s + N_R^R)]$	$N_T^S N_R^R [\frac{\alpha(\lambda-1)(\alpha+1)}{2} + 74\mu$ $+ \frac{7T^3+15T^2+2T}{6}]$ $+T[N_s (N_R^R - 1) + N_T^R (N_s + N_R^R - 2)]$	$N_T^S N_R^R [\frac{\alpha(\alpha+1)}{2} (2\lambda - 1)$ $+ 94\mu + \frac{7T^3+12T^2-T}{3}]$ $+T[N_s (2N_R^R + 2N_T^R - 1) + N_R^R (N_T^R + 1) - 2N_T^R]$

It should be verified that the A&F relay node presents less computational complexity, where $N_T^R N_R^R T$ and $N_T^R T (N_R^R - 1)$, multiplications and summations, respectively, are required. In addition, both D&F with PCE and LS relay nodes perform stages of decoding and encoding processes, which increase the complexity. From Table 4, it should be highlighted that $N_T^R \times N_R^R$ is the combiner antennas in the NR-relay nodes and $\lambda \times \alpha = P$ explains the total number of the pilot symbols. Additionally, μ represents the total number of the data symbols, which are employed to implement the interpolate method. Considering this, the D&F with PCE has knowledge of the radio channel, the complexity of the protocol decreases, substantially, in comparison with D&F with LS, due to the channel estimation and interpolation algorithms are not performed in the decoding step. Accordingly, $N_T^S N_R^R [\frac{\alpha(\alpha+1)}{2} (\lambda + \alpha - 1) + 94\mu]$ fewer operations are required achieved with this strategy.

The KPIs of the co-operative system have been studied in previous works, which consider a similar architecture, using the network model, frequencies bands, and hardware approach. In this context, a brief comparison with prior works [31–33] is performed. The first conclusion of these works is that the D&F relay node is able to achieve higher performance compared to the A&F. Nevertheless, the main limitation found in these works is the implemented signal model, which does not fulfill the 5G 3GPP requirements—for example, the physical uplink shared channel, as proposed in this paper. Furthermore, this work focuses the simulator through a hardware implementation of the uplink relay nodes by means of the design of mmWave transceptor (Tx/Rx). On the other hand, the disadvantages of our proposed method are the half duplex mode in the architecture and fixed scenario. Nevertheless, full duplex operation and mobility in 5G network will be addressed in further research.

5. Conclusions

In this paper, the uplink in a two-hop 5G new radio co-operative system in millimeter bands has been simulated and studied, based on practical assumptions in terms of system and network implementation. For the millimeter band operation of relay nodes, 26 GHz Tx/Rx chains have been designed and implemented. An indoor-to-outdoor scenario has been considered. Two relaying strategies have been studied: an RN amplify-and-

forward relay node (A&F RN) and RN decode-and-forward relay node (D&F RN). For the decode-and-forward strategy, two schemes have been analyzed and implemented. The first one considers channel knowledge (PCE) to perform the decoding and encoding stages and the second one takes into account the practical channel estimation through the Least Square (LS) estimator. The 5G NR uplink signal fulfills the requirements standardized by the 3GPP and SISO and MIMO schemes have also been considered. A hardware implementation of the co-operative network and relay nodes has been simulated at the link level using Matlab™ and Simulink™ commercial software.

Key performance indicators (KPIs) of the uplink mmWave NR-RNs have been studied and analyzed. The numerous results obtained from the Monte-Carlo simulation of the system showed that a two-hop uplink mmWave NR-RN co-operative system can greatly improve the average performance of the communications between the User Equipment (UE) and gNodeB. The obtained results demonstrate that the key performance indicators obtained by uplink mmWave NR A&F protocol are lower than the those obtained via the uplink mmWave NR D&F strategy. Furthermore, it can be concluded that the NR D&F PCE algorithm presents a higher average performance than the NR D&F LS protocol. For example, the maximum throughput of the proposed NR D&F PCE algorithm with the SISO antenna technique and 64-QAM constellation is 15.83 Mbps at SNR = 20 dB; however, taking into account the NR D&F LS strategy, the reached average throughput is lower, by approximately 13.23 Mbps. It can be noted that the uplink mmWave NR-RN co-operative system with MIMO technology led to a considerable average performance in terms of the indoor-to-outdoor communication, which achieved higher KPIs in the 256-QAM signal. In addition, it was demonstrated that D&F relay node presents high computational complexity in comparison with A&F and the proposed co-operative simulator, which is a topic not deeply addressed in related research. Additionally, this paper introduces the first step for the implementation of the uplink mmWave MIMO NR-RN co-operative network through Matlab™ and Software Defined Radio (SDR), which will be followed up on by our research team.

Author Contributions: R.V.-P. conceived the paper, designed the experiments, performed experiments, analyzed the data, and wrote the paper; R.V.-P. and J.I.A. reviewed and edited the paper. Both authors have read and agreed to the published version of the manuscript.

Funding: This work was supported by the Spanish Ministry of Science, Innovation and Universities within the project TEC2017-87061-C3-1-R (CIENCIA/AEI/FEDER, UE). The work of Randy Verdecia-Peña is supported by a pre-doctoral Contract PRE2018-085032 from the Ministry of Science and Innovation.

Institutional Review Board Statement: Not applicable.

Informed Consent Statement: Not applicable.

Data Availability Statement: Data sharing not applicable.

Conflicts of Interest: The authors declare no conflict of interest.

References

1. Agiwal, M.; Roy, A.; Saxena, N. Next Generation 5G Wireless Networks: A Comprehensive Survey. *IEEE Commun. Surv. Tutor.* **2016**, *18*, 1617–1655. [[CrossRef](#)]
2. Shaikh, A.; Kaur, M.J. Comprehensive Survey of Massive MIMO for 5G Communications. In Proceedings of the 2019 Advances in Science and Engineering Technology International Conferences (ASET), Dubai, United Arab Emirates, 26 March–10 April 2019; doi:10.1109/ICASET.2019.8714426. [[CrossRef](#)]
3. Gao, Z.; Dai, L.; Mi, D.; Wang, Z.; Imran, M.A.; Shakir, M.Z. mmWave Massive-MIMO-based Wireless Backhaul for the 5G Ultra-Dense Network. *IEEE Wirel. Commun.* **2015**, *22*, 13–21. [[CrossRef](#)]
4. Darsena, D.; Gelli, G.; Iudice, I.; Verde, F. Separable MSE-Based Design of Two-Way Multiple-Relay Cooperative MIMO 5G Networks. *Sensors* **2020**, *20*, 6284. [[CrossRef](#)] [[PubMed](#)]
5. Adnan, M.H.; Ahmad Zukarnain, Z. Device-To-Device Communication in 5G Environment: Issues, Solutions, and Challenges. *Symmetry* **2020**, *12*, 1762. [[CrossRef](#)]

6. Salam, T.; Rehman, W.U.; Youssef, A. Data Aggregation in Massive Machine Type Communication: Challenges and Solutions. *IEEE Access* **2019**, *7*, 41921–41946. [[CrossRef](#)]
7. Jaffry, S.; Hussain, R.; Gui, X.; Hasan, S.F. A Comprehensive Survey on Moving Networks. *IEEE Commun. Surv. Tutor.* **2021**, *23*, 110–136. [[CrossRef](#)]
8. Kamel, M.; Hamouda, W.; Tao, X. Ultra-Dense Networks: A Survey. *IEEE Commun. Surv. Tutor.* **2016**, *18*, 2522–2545. [[CrossRef](#)]
9. Siddiqi, M.A.; Yu, H.; Joung, J. 5G Ultra-Reliable Low-Latency Communication Implementation Challenges and Operational Issues with IoT Devices. *Electronics* **2016**, *8*, 981. [[CrossRef](#)]
10. Rappaport, T.S.; Xing, Y.; MacCartney, G.R.; Molisch, A.F.; Mellios, E.; Zhang, J. Overview of Millimeter Wave Communications for Fifth-Generation (5G) Wireless Networks—With a Focus on Propagation Models. *IEEE Trans. Antennas Propag.* **2017**, *65*, 6213–6230. [[CrossRef](#)]
11. Uwaechia, A.N.; Mahyuddin, N.M. A Comprehensive Survey on Millimeter Wave Communications for Fifth-Generation Wireless Networks: Feasibility and Challenges. *IEEE Access* **2020**, *8*, 62367–62414. [[CrossRef](#)]
12. Albream, M.A.; Juntti, M.; Shahabuddin, S. Massive MIMO Detection Techniques: A Survey. *IEEE Commun. Surv. Tutor.* **2019**, *21*, 3109–3132. [[CrossRef](#)]
13. Busari, S.A.; Huq, K.M.S.; Mumtaz, S.; Dai, L.; Rodriguez, J. Millimeter-Wave Massive MIMO Communication for Future Wireless Systems: A Survey. *IEEE Commun. Surv. Tutor.* **2018**, *20*, 836–869. [[CrossRef](#)]
14. Taori, R.; Sridharan, A. Point-to-multipoint in-band mmwave backhaul for 5G networks. *IEEE Commun. Mag.* **2015**, *53*, 195–201. [[CrossRef](#)]
15. Chataut, R.; Akl, R. Massive MIMO Systems for 5G and beyond Networks—Overview, Recent Trends, Challenges, and Future Research Direction. *Sensors* **2020**, *20*, 2753. [[CrossRef](#)] [[PubMed](#)]
16. Hossain, M.A.; Md Noor, R.; Yau, K.-L.A.; Ahmedy, I.; Anjum, S.S. A Survey on Simultaneous Wireless Information and Power Transfer With Cooperative Relay and Future Challenges. *IEEE Access* **2019**, *7*, 19166–19198. [[CrossRef](#)]
17. Verdecia-Peña, R.; Alonso, J.I. A Comparative Experimental Study of MIMO A&F and D&F Relay Nodes Using a Software-Defined Radio Platform. *Electronics* **2021**, *10*, 570. [[CrossRef](#)]
18. Verdecia-Peña, R.; Alonso, J.I. A Two-Hop mmWave MIMO NR-Relay Nodes to Enhance the Average System Throughput and BER in Outdoor-to-Indoor Environments. *Sensors* **2021**, *21*, 1372. [[CrossRef](#)]
19. 3GPP, “5G; NR; Physical layer procedures for data”. *ETSI TS* **2018**, *38.214*, 15.
20. 3GPP, “5G; NR; Physical channels and modulation”. *ETSI TS* **2018**, *38.211*, 15.
21. Mathworks, “nrCDLChannel, Send Signal through CDL Channel Model”. Available online: <https://es.mathworks.com/help/5g/ref/nrcdlchannel-system-object.html/> (accessed on 1 December 2020).
22. 3GPP, “5G; Study on channel model for frequencies from 0.5 to 100 GHz”. *ETSI TS* **2017**, *138.901*, 14.
23. Analog Devices, Mini Circuits, Gali-84+, Monolithic Amplifier, DC-6 GHz. Available online: <https://www.xmicrowave.com/product/xm-a114-0404c/> (accessed on 1 December 2020).
24. Analog Devices, HMC292ALC3B, GaAs Double Balance Mixer, 14 to 30 GHz. Available online: <https://www.xmicrowave.com/product/xm-a4j1-0404c/> (accessed on 1 December 2020).
25. Analog Devices, ADF5355PLL, Microwave Wideband Synthesizer with Integrated VCO. Available online: <https://www.xmicrowave.com/product/xm-a741-0409c-01/> (accessed on 1 December 2020).
26. Analog Devices, HMC576LC3B, SMT GaAs MMiC × 2 Active Frequency Multiplier, 18 to 29 GHz Output. Available online: <https://www.xmicrowave.com/product/xm-a3d9-0404c-01/> (accessed on 1 December 2020).
27. Analog Devices. HMC499LC4, SMT PHEMT Medium Power Amplifier, 21–32 GHz. Available online: <https://www.xmicrowave.com/product/xm-a515-0404c-01/> (accessed on 1 December 2020).
28. Analog Devices, HMC944APM5E, GaAs PHEMT MMiC Power Amplifier, DC-28 GHz. Available online: <https://www.xmicrowave.com/product/xm-a266-0804c-01/> (accessed on 1 December 2020).
29. Pasternack, PE9851/2F, WR-34 Waveguide Standard Gain Horn Antenna Operating from 22 GHz to 33 GHz, with 20 dB. Available online: <https://www.pasternack.com/standard-gain-horn-waveguide-size-wr34-20-db-gain-292mm-female-pe98512f-20-p.aspx> (accessed on 6 December 2020).
30. Analog Devices, HMC519LC4, GaAs PHEMT MMiC Low Noise Amplifier, 18 to 31 GHz. Available online: <https://www.xmicrowave.com/product/xm-a373-0404c-01/> (accessed on 1 December 2020).
31. Calle-Sanchez, J.; Martinez-de-Rioja, E.; Molina-Garcia, M.; Alonso, Jose I. Performance of LTE Mobile Relay Node Usage for Uplink Access in High Speed Railway Scenarios. In Proceedings of the 2015 IEEE 81st Vehicular Technology Conference (VTC Spring), Glasgow, UK, 14 May 2015; doi:10.1109/VTCspring.2015.7146012. [[CrossRef](#)]
32. Lohani, S.; Loodaricheh, R.A.; Hossain, E.; Bhargava, V.K. On Multiuser Resource Allocation in Relay-Based Wireless-Powered Uplink Cellular Networks. *IEEE Trans. Wirel. Commun.* **2016**, *15*, 1851–1865. [[CrossRef](#)]
33. Zhang, Z.; Ma, Z.; Xiao, M.; Karagiannidis, G.K.; Ding, Z.; Fan, P. Two-Timeslot Two-Way Full-Duplex Relaying for 5G Wireless Communication Networks. *IEEE Trans. Commun.* **2016**, *64*, 2873–2887. [[CrossRef](#)]

Short Biography of Authors



Randy Verdecia-Peña (S'14-M'19) was born in Granma, Cuba, in 1991. He received a degree in Telecommunications and Electronics Engineer from the University of Oriente (Higher Polytechnic Institute Julio Antonio Mella), Santiago of Cuba, Cuba, in 2014. He received M.Sc. degree in Electrical Engineering from the Pontifical Catholic University of Rio de Janeiro (PUC-Rio), Brazil, in 2019. From 2014 to 2017, he worked with the Telecommunications Company of Cuba (ETECSA) as specialist in telematics. His research interests are in communications system, data networks and satellites. He is currently working toward the Ph.D. degree. In 2017 he received a CAPES scholarship from Education Ministry, Brazil. He is currently working with the Department of Information Processing and Telecommunications Center, UPM. His research studies have included solutions for the physical layer of the future fifth generation of mobile communication systems (5G). He has also worked with the 3GPP standard in the solutions of New Generation Networks. He is currently involved in the study of new technologies and their implementation in High-Speed Railways (HSR) for 4G and 5G communications. He has received a scholarship from the Science, Innovation and University Ministry, Spain.



José I. Alonso (M'91) received a degree in Telecommunications Engineering, as well as a Ph.D., from the Technical University of Madrid (UPM). Dr. Alonso began his career at Telettra España, S.A., as microwave design engineer. He then joined the Department of Signals, Systems, and Radiocommunications at UPM, where he is currently a Full Professor. His research has included the analysis and simulation of high-speed/high-frequency integrated circuits and their interconnections, as well as the computer-aided design and measurement of hybrid and GaAs monolithic microwave integrated circuits (MMICs) and their applications in the development and implementation of mobile, optical fiber, and communications systems. He has also worked in the development and radio planning of broadband point-multipoint radio systems (LMDS) in millimetre frequencies and wireless and mobile communications systems (WiFi, WiMAX, TETRA, GSM-R, and LTE). He is involved in the study of the viability of the use of 5G communications for critical communications and operational and passenger services in rail environments; in particular, its potential applicability to the FRMCS, in co-operative communications in 5G systems, and the development of localization techniques based on femtocell LTE networks. He has participated in more than 90 research projects and contracts financed by national and international institutions and companies. He has authored more than 200 publications in scientific journals, symposium proceedings, seminars, and reports. In addition, he holds three patents.